Sea ice outlook in 2012: Summer atmospheric and sea ice dynamical contributions to fall sea ice extent

July Report based on June Data

J.V. Lukovich, M.G. Asplin, D.G. Babb, B. Horton, and D.G. Barber
Centre for Earth Observation Science (CEOS)
University of Manitoba

Estimate for sea ice extent for September, 2012; comparable to or less than the 2011 minimum in sea ice extent, or 4.33 million square kilometers.

Executive Summary

It is hypothesized that the 2012 fall sea ice extent will achieve values comparable to those of 2011 based on a heuristic assessment of sea ice and atmospheric dynamics, with regional losses governed by local wind and ice conditions and dynamics.

Rationale

Similarity in stratospheric and surface wind patterns in 2007, 2011 (years associated with a record low in sea ice extent) and 2012 in contrast to 2009 when a partial recovery in sea ice was observed, suggest atmospheric dynamical contributions conducive to increased summer export of sea ice through Fram Strait in a manner consistent with recent studies illustrating dominant role of wind anomalies in governing summertime sea ice extent (Ogi and Wallace, 2012). Ice concentrations and ice drift in May illustrate a continued decrease in ice concentrations, particularly in the Beaufort Sea, and enhanced anticyclonic circulation to the north of Bering Strait that provides the mechanism for ice export from the east Siberian Sea. Ice concentration in June shows a decrease of ice concentrations in the Beaufort Sea, Hudson Bay, and Baffin Bay, while nowcast data show a decrease in ice thickness at the pack ice edge that suggests increased sensitivity of the ice cover to ice melt and sea ice deformation during summer. Furthermore, daily maps of surface winds, SLP and nowcast ice drift in June illustrate increased variability in ice drift and regional differences in ice drift response to surface wind forcing.

Discussion

As for the May SIO assessment, similarity in stratospheric relative vorticity fields for March, 2007, 2011, and 2012, and dissimilarity with those for 2009 associated with a partial recovery in sea ice extent indicate upper-level atmospheric conditions that are favourable to a continued loss in sea ice extent (Figure 1). In particular, a dipolar configuration with maximum anticyclonic activity located over the Beaufort Sea and cyclonic activity over the North Atlantic is observed in 2007, 2011, and 2012, with an eastward shift in the dipolar interface in 2012 that may have implications for ice drift near Bering Strait and contributions to the transpolar drift from the western Arctic. Maximum surface winds and positive anomalies near Fram Strait in May, 2007, 2011, and 2012 in contrast to 2009 indicate wind conditions conducive to increased summer export through Fram Strait via the transpolar drift stream (Figure 2), in a manner consistent with recent studies highlighting the dominant role of atmospheric wind anomalies in summertime sea ice extent (Ogi and Wallace, 2012)

An assessment of ice concentrations and drift in May, 2007, 2011, and 2012 (the last month for which monthly averages of ice drift are available) illustrates a continued decrease in ice concentrations and ice export through Fram Strait, with variability in the strength and location of the Beaufort Gyre and Transpolar Drift between years (Figure 3). Of particular interest are ice concentrations in the southern Beaufort Sea, which exhibits a larger expanse of open water in 2012, and increased spatial coverage of lower ice concentrations. Noteworthy also in 2012 is a poleward migration in the TPD and enhanced anticyclonic circulation north of the Bering Strait that will advect ice from the east Siberian Sea.

SSMIS ice concentration and nowcast ice thickness data on June 30th, 2012 show a continued decline in ice concentrations in the southern Beaufort Sea, Hudson Bay, and Baffin Bay, accompanied by a decrease in ice thickness in the Beaufort Sea poleward of 80N, and near the ice edge (Figure 4). The Laptev Sea is also covered by sea ice at this time, in contrast to 2011. The absence of a filament of thick ice to the north of the east Siberian Sea in 2012 in contrast to 2011 suggests the removal of a barrier that would otherwise hinder advection and transport of ice for export through Fram Strait. Decreases in ice thickness at the pack ice edge further suggest increased sensitivity to ice melt and sea ice deformation during summer that will contribute to accelerated loss of sea ice in September.

Daily maps of surface winds, SLP, and nowcast ice drift data illustrate regional differences in atmospheric forcing of sea ice in 2011 and 2012 (Figures 5 and 6). Noteworthy are maximum ice drift speeds through Fram Strait in early June, 2012 aligned with the interface between the SLP high and low regimes, observed to a lesser extent in late June of 2011. Increased variability in ice drift is also observed in 2012 compared to 2011. It is interesting to note that the anticyclonic circulation in the Beaufort Sea is preceded by a SLP high on June 14th, 2012, suggesting regional differences in ice drift response to surface winds, most likely due to regional differences in ice concentration and thickness.

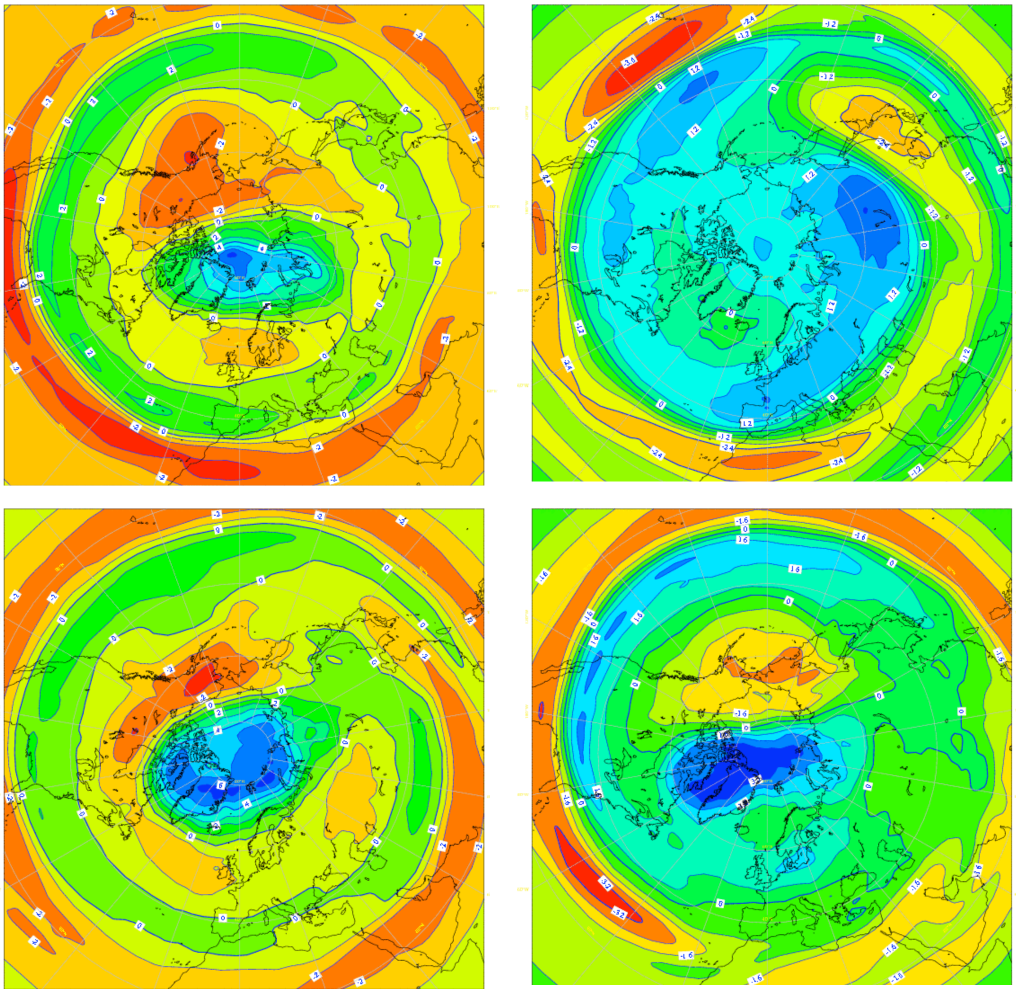

Figure 1. Stratospheric (10 mb) relative vorticity fields for (clockwise from upper left corner) March, 2007, 2009, 2011 and 2012. Anticyclonic activity (negative relative vorticity) is depicted by red shading. Image provided by the ECMWF ERA-Interim data portal at http://data-portal.ecmwf.int/data/d/interim_moda/levtype=pl/.

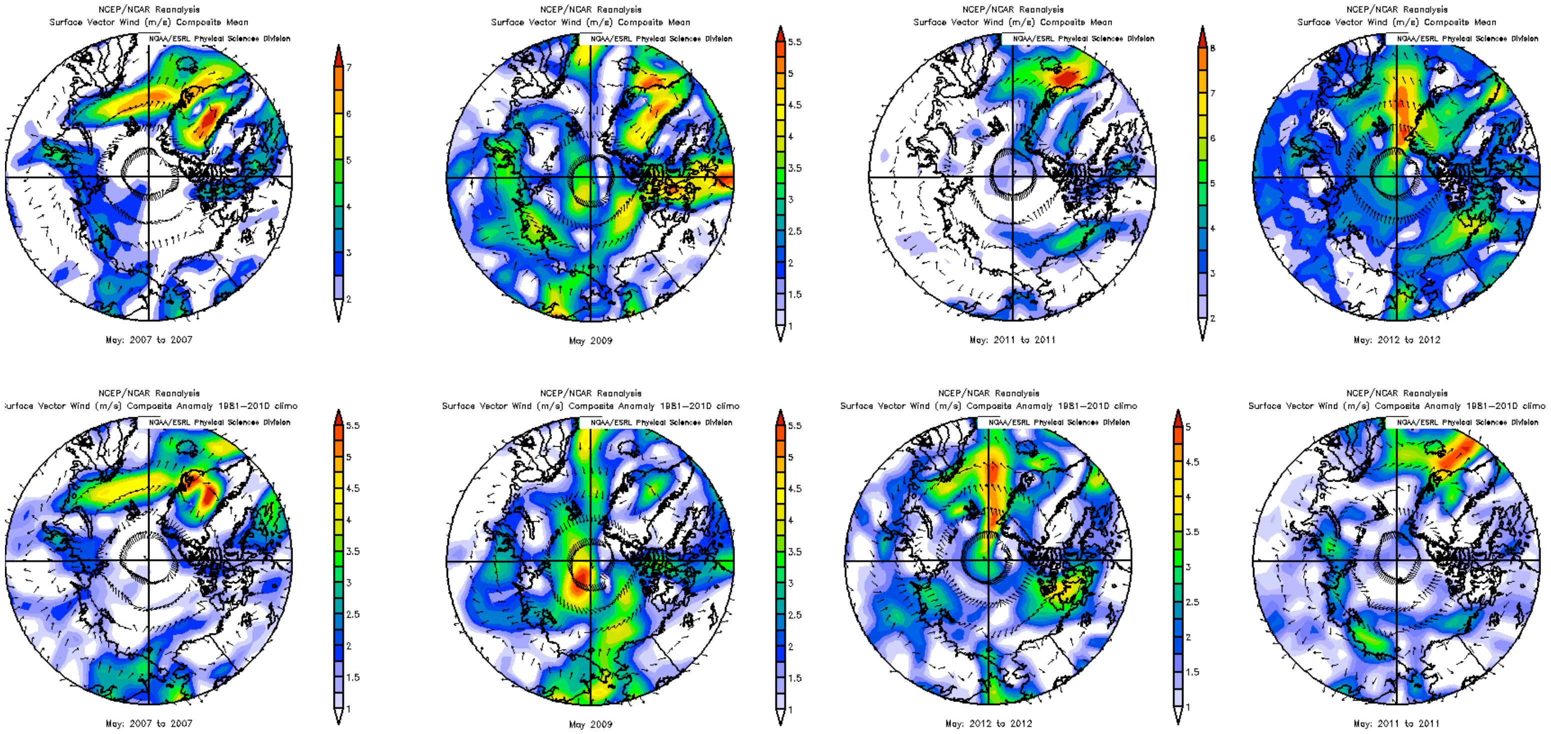

Figure 2. Surface winds and anomalies for May, 2007, 2011, and 2012. Image provided by the NOAA/ESRL Physical Sciences Division, Boulder Colorado from their Web site at http://www.esrl.noaa.gov/psd/.

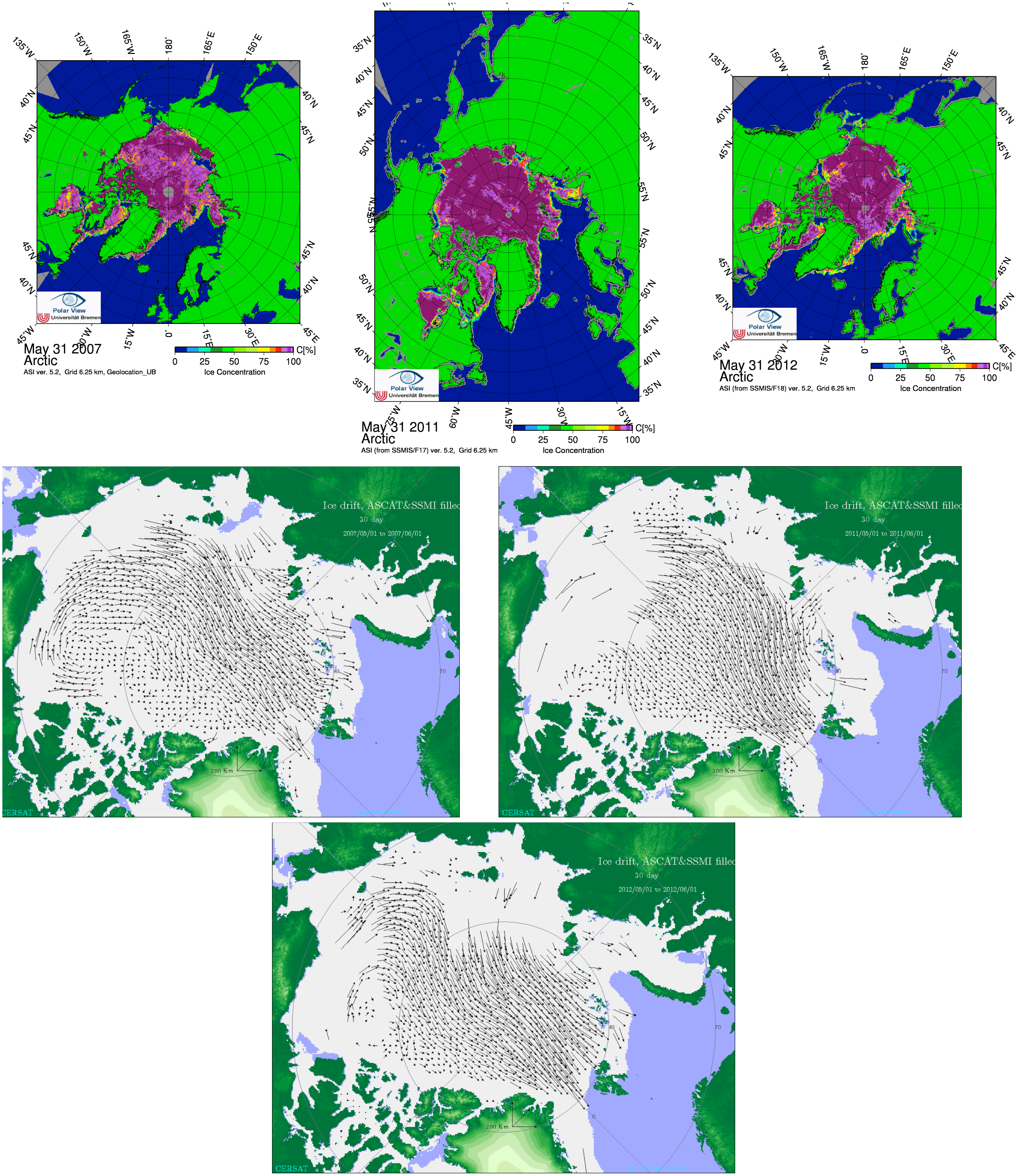

Figure 3. AMSR-E maps of sea ice concentration in the Arctic for May 31st in 2007, 2011, and 2012 in addition to monthly sea ice drift for May 2007, 2011, and 2012. Sea ice concentration image provided by the University of Bremen at http://www.iup.uni-bremen.de:8084/amsr/, and sea ice drift image provided by Institut Francais de recherche pour l'exploitation de la mer at ftp://ftp.ifremer.fr/ifremer/cersat/products/gridded/psi-drift/quicklooks/arctic/.

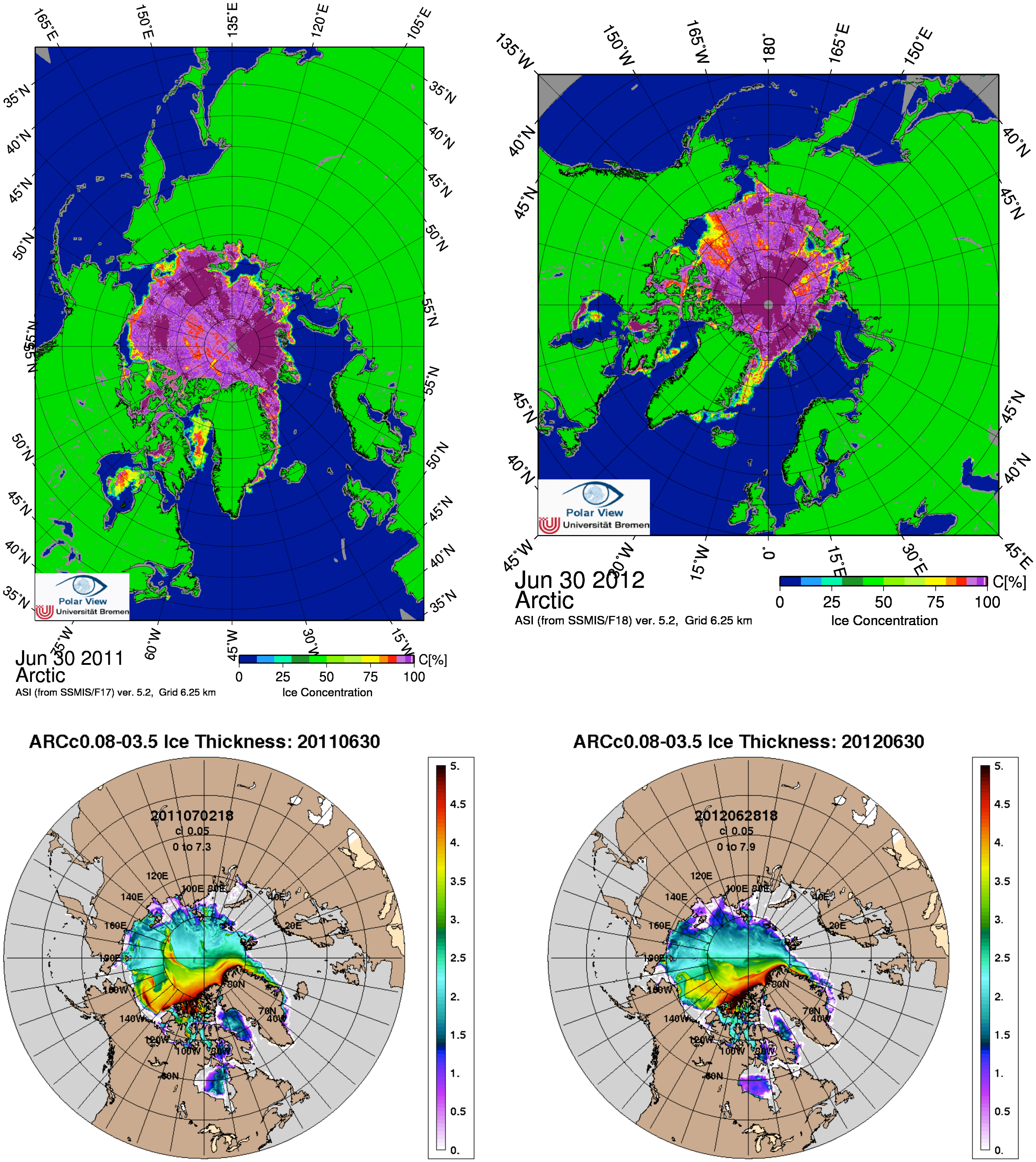

Figure 4. Upper row: AMSR-E sea ice maps of sea ice concentrations in the Arctic for June 30th, 2011 and 2012. Image provided by the University of Bremen at http://www.iup.uni-bremen.de:8084/amsr/.
Lower row: Arctic sea ice thickness nowcast from the Naval Research Laboratory (NRL) – HYCOM Consortium for Data-Assimilative Ocean Modeling. Image provided by the Naval Research Laboratory at http://www7320.nrlssc.navy.mil/hycomARC/navo/arcticictn/nowcast/.

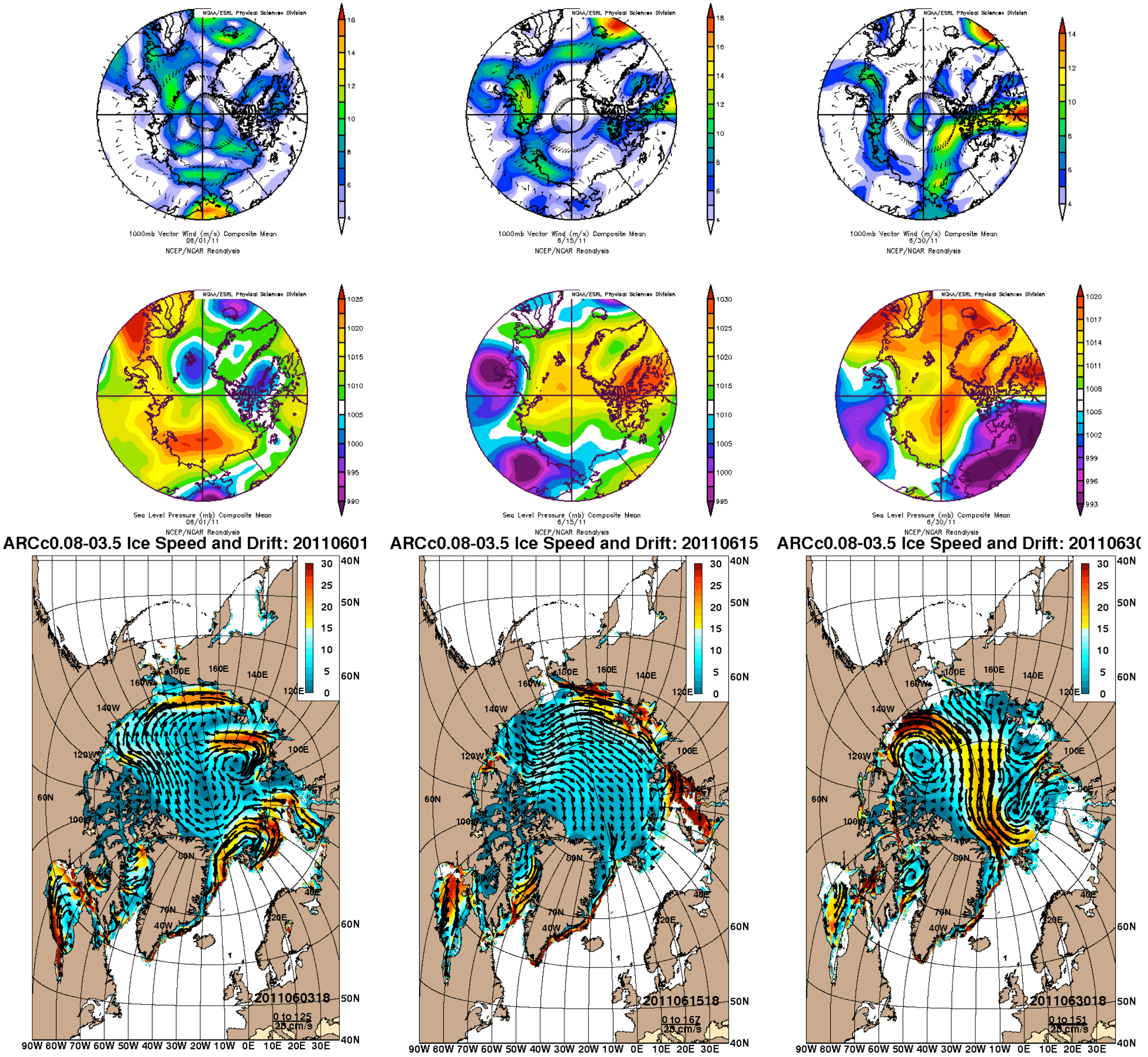

Figure 5. Surface winds (top row), SLP (middle row), and nowcast ice drift (lower row) for June 1st, 15th, and 30th, 2011. Image for surface winds and SLP provided by the NOAA/ESRL Physical Sciences Division, Boulder Colorado from their Web site at http://www.esrl.noaa.gov/psd/, and nowcasts obtained from the Naval Research Laboratory (NRL) – HYCOM Consortium for Data-Assimilative Ocean Modeling at http://www7320.nrlssc.navy.mil/hycomARC/navo/arcticictn/nowcast/.

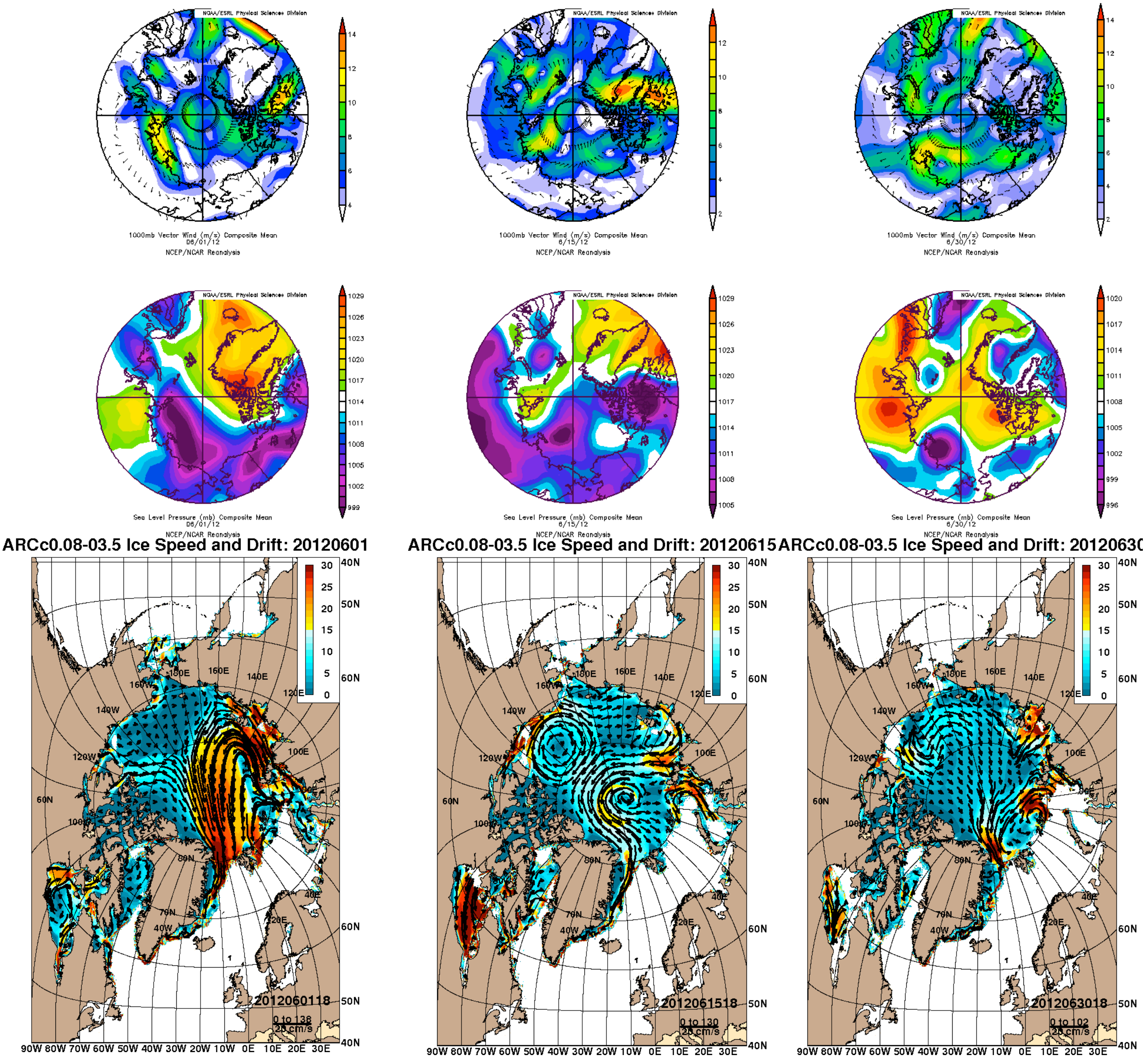

Figure 6. Surface winds (top row), SLP (middle row), and nowcast ice drift (lower row) for June 1st, 15th, and 30th, 2012. Image for surface winds and SLP provided by the NOAA/ESRL Physical Sciences Division, Boulder Colorado from their Web site at http://www.esrl.noaa.gov/psd/, and nowcasts obtained from the Naval Research Laboratory (NRL) – HYCOM Consortium for Data-Assimilative Ocean Modeling at http://www7320.nrlssc.navy.mil/hycomARC/navo/arcticictn/nowcast/.